



FUPRE Journal

of

Scientific and Industrial Research








ISSN: 2579-1184(Print)

ISSN: 2578-1129 (Online)

<http://fupre.edu.ng/journal>

Modelling of Average Weight Loss in Welding Defects using Response Surface Methodology and Artificial Neural Network

MABIAKU, T.A.¹ , ACHEBO, J. I.¹ , ²OBAHIAGBON, K. O.² , OZIGAGUN, A.,¹ 
, UWOGHIREN, F. O.^{1,*} 

¹Department of Production Engineering, University of Benin, Benin City, Nigeria.

²Department of Chemical Engineering, University of Benin, Benin City, Nigeria.

ABSTRACT

ARTICLE INFO

Received: 10/01/2024
Accepted: 10/05/2024

Keywords

Artificial Neural Network, Average weight loss, Pipeline weldments, Response Surface methodology

The study aims to bridge this gap by scrutinizing the impact of a specific non-elastic factor, namely the average weight loss, on pipeline weldments and its interaction with elastic properties. To fulfil this objective, a comprehensive experimental inquiry is conducted, encompassing diverse welding methods, materials, and environmental conditions to authentically replicate real-world situations. This investigation unveils the intricate interrelation between elastic and non-elastic facets, underscoring the necessity of encompassing the latter to ensure the dependability of pipeline weldments across various operational contexts. Cutting-edge techniques, such as machine learning algorithms and finite element simulations, are harnessed to accurately predict and optimize these non-elastic factors, thereby enhancing the overall strength and structural integrity of pipeline weldments. The experimental setup adheres to the central composite design, meticulously constructed utilizing design expert software (version 13.0). The response surface methodology analysis yields optimal outcomes, suggesting a gas flow rate of 14.667 liters per minute, a voltage of 21.280 volts, and a current of 160.000 amps. These parameters collectively yield a welded joint with an average weight loss value of 0.236, achieving a desirability value of 0.918. Additionally, the artificial neural network model is employed to predict output parameters and compared against the RSM methodology. The findings underscore the pivotal role of optimizing non-elastic performance factors in pipeline weldments. By accurately anticipating and controlling the period of immersion, engineers and professionals within the pipeline sector can design weldments capable of enduring harsh conditions, thus, prolonging pipeline operational lifespans.

1. INTRODUCTION

The structural integrity of pipeline weldments is a crucial factor in ensuring the safety and reliability of various industries, including oil and gas, petrochemicals, and

energy transportation (Jiang, 2018). Achieving optimal structural integrity requires a comprehensive understanding of the factors that influence weld quality (Dogra, 2018). This research focuses on

*Corresponding author, e-mail:author@fupre.edu.ng

DIO

©Scientific Information, Documentation and Publishing Office at FUPRE Journal

investigating the role of average weight as a factor in enhancing the structural integrity of pipeline weldments, exploring relevant studies, methodologies, and findings. Weldments play a vital role in the structural integrity of pipelines, and several factors impact their quality (Cheng and Chen, 2022; Li et al., 2019). These factors include welding parameters, material properties, environmental conditions, and geometrical characteristics (Alzeer et al., 2023). While these factors have been extensively studied, the consideration of average weight as a distinct factor and its influence on weldment integrity is an emerging research area. Weight, or more specifically, the mass of the components being welded, can significantly influence the welding process and subsequent structural integrity (Seyfipour et al., 2023). The weight affects heat distribution, cooling rates, thermal stresses, and distortion during welding (Sabdin et al., 2019). The consideration of average weight as a controlling parameter can provide valuable insights into the complex interactions between weight and weldment integrity.

Impacts of Weight on Residual Stresses and Distortion: Several studies have highlighted the influence of weight on residual stresses and distortion in welded structures. Heavier components tend to retain heat longer, potentially leading to higher residual stresses and increased distortion (Spoerk et al., 2020). Research by Zhao et al. (2023) emphasized the importance of accounting for weight-related effects on residual stresses and distortion to ensure the long-term structural integrity of welded pipelines. Weight can also affect the microstructure of the weldment due to variations in cooling rates and thermal cycles (Li et al., 2020). These microstructural changes can impact material properties, such as hardness, toughness, and susceptibility to cracking (Fernandes et al.,).

The work of Liu (2021) investigated weight-induced changes in microstructure and mechanical properties, further underlining the need to model average weight as a factor in weldment integrity analysis. Numerical modelling approaches, such as computational fluid dynamics (CFD) and finite element analysis (FEA), have been used to study the effects of average weight on weldments. These models simulate heat distribution, cooling rates, and resulting stresses and strains (Miranda and Nogueira, 2019). Integrating average weight as a variable in these models can provide a quantitative understanding of its impact on weldment integrity (Linda and Pistorius, 2022). While the importance of average weight in weldment integrity is recognized, more research is needed to develop comprehensive models that consider weight alongside other influencing factors (Cecchel, 2021). The integration of average weight into advanced modelling techniques, such as Multiphysics simulations, can provide a holistic understanding of its role in weldment integrity and guide practical applications (Ardil, 2023).

In conclusion, the present study highlights the growing significance of modelling average weight as a factor in augmenting the structural integrity of pipeline weldments. Weight affects heat distribution, residual stresses, distortion, and microstructural changes, all of which impact the quality of welded joints. Incorporating average weight as a controlling parameter in numerical models can contribute to a deeper understanding of its influence and aid in the development of pipelines with improved structural integrity. Further research is warranted to refine modelling techniques, validate findings through experiments, and translate these insights into practical applications for industries that rely on welded pipelines.

2. METHODOLOGY

2.1. Process parameters

In this research study, several variables were investigated in relation to the temperature of the welding pool. These variables included welding voltage, gas flow rate, and current. To carry out the experiments, twenty runs were conducted with varying combinations of welding voltage, gas flow rate, and current, and these runs were utilized to connect two mild steel plates, each spanning 60 x 40 x 10 mm. To assess the hardness of the resulting welds, the Brinell hardness test was performed using a specialized Brinell hardness testing unit. This test involves the use of a tungsten carbide ball with a specific diameter (D). The ball is subjected to a predetermined force (F), held in place for a specified duration (T), and then released. As a result of this process, the spherical indenter creates a permanent deformation or imprint on the tested metal piece. Averaging measurements made at two or more places inside the indentation yields the indentation's diameter (d). To execute the Brinell hardness test, The body of the Brinell Hardness Testing Machine is enclosed by a system consisting of a loading system encompassing levers, weights, a hydraulic dashpot, and a plunger. The test material is positioned on the movable anvil. When the lever is engaged, the spherical ball indenter descends onto the material, exerting a predefined force which is subsequently displayed and analysed on the screen.

2.2 Design of Experiment

The design of experiments (DOE) is a procedure that is systematic and scientific for planning and conducting tests to establish a cause-and-effect relationship between variables. It is also a rigorous approach for manipulating the input factors of a process

and observing the resulting outcomes while considering the random variability inherent in the process. Experimentation is a crucial component of scientific research, and computer tools like Design Expert and Minitab play a significant role in facilitating this process. These software programs aid in collecting data through experimental techniques to ensure precise polynomial approximations. Various types of experimental designs are available, including full factorial, Latin hypercube, central composite circumscribed, and central composite face-centred designs.

Design Expert software was used to generate the experimental matrix for this investigation, and the central composite design (CCD) was selected as the experimental design. The CCD follows the mathematical process outlined in equation (1).

$$N = 2^n + 2n + k \quad (1)$$

Where N = Total number of experiments, n = number of input parameters.

The quantity of input parameters taken into consideration had an impact on the choice of the central composite design for running experiments. In this research, models for all the responses were generated using Design Expert software.

2.3 Materials and Experimental Set-up

In the gas tungsten arc welding (GTAW) system, which operated within a current range of 150 to 200 A, thermocouples were affixed. This welding process was applied to a low-carbon steel block measuring 200 x 200 x 20 mm³. A DCEN (Direct Current Electrode Negative) setup with a 4 mm-arc gap was employed for shielding the gas. Temperature measurements were taken in the range of 1500 to 1800 °C. W5 tungsten

thermocouples were used for their excellent resistance to high temperatures. These thermocouples had an overall diameter of 1.2 mm, which included both the sleeving and tungsten wires. They were placed into the samples at a depth of 4 mm, with a diameter of 1.4 mm and an angle of 20°.

2.4 Method of Data Collection

The Design Expert software generated a central composite design matrix, and based on this matrix, twenty test runs were conducted. These test runs included the results of the weld sample, along with input and output parameters. The size of the data matrix was determined using the formula $2n + 2n + k$, where k stands for the number of center points, $2n$ for axial points, and $2n$ for factorial points. Subsequently, Artificial Neural Network (ANN) and Response Surface Methodology (RSM) techniques were used to analyze this matrix.

2.5 Response Surface Methodology

Engineers frequently utilize Response Surface Methodology (RSM) to identify the ideal circumstances required to carry out a certain activity. This involves identifying the input parameter values for a process that result in the best possible outcomes, whether it's minimizing or maximizing a particular parameter. RSM is a widely used optimization technique that helps engineers understand how a process works by utilizing mathematical and statistical methods to model and predict the desired response.

2.6 Artificial Neural Network

A neural network is a highly parallel and distributed computer system that possesses the capability to store experimental data for various applications. It functions as a data

mining tool and is primarily designed to uncover hidden patterns within datasets. Interestingly, there are two key similarities between neural networks and the human brain. First, during the learning process within the network, synaptic weights are employed to store knowledge. These weights indicate the strength of connections between internal neurons. Second, each basic neuron with R inputs receives appropriate weights (w), and the transfer function (f) calculates the sum of these weighted inputs along with a bias term. The transfer function (f) can be any differentiable function used to determine neuron outputs. In multilayer networks, the log-sigmoid transfer function, often referred to as logsig, is a commonly employed choice. The sigmoid transfer function, specifically the log-sigmoid, generates output values that range from 0 to 1 as the neuron's net input changes from a negative number to a positive infinity.

3. RESULTS AND DISCUSSION

3.1. Presentation of results

3.1.1. Modelling of the Average Weight Loss (AWL) using Response Surface Methodology (RSM)

In this research, current (I), voltage (V), and gas flow rate (GFR) are chosen as the input variables, and an effort is made to construct a second order mathematical relationship between them, coupled with one response variable, average weight loss using response surface methodology (RSM).

The optimization model's goal was to reduce the average weight loss.

The end result of the optimization method was to identify the current (Amp), voltage (Volt), and gas flow rate (l/min) ideal values that will minimize average weight loss.

To produce the experimental information needed for the optimization process;

- i. The central composite design approach (CCD) was used for the statistical design of the experiment (DOE). A statistical tool was used to carry out the design and optimization. It was decided to use Design Expert 7.01 for this specific issue.

- ii. A second step involved creating an experimental design matrix with 20 experimental runs and six (6) center points (k), six (6) axial points (2n), and eight (8) factorial points (2n).

To validate how well the quadratic model fits the data in analyzing the experimental data, the sequential model sum of squares was estimated for the typical response to weight loss, as shown in Table 1.

Table 1: Sequential model sum of square for Average Weight Loss

Source	Sum Squares	of df	Mean Square	F-value	p-value	
Mean vs Total	1.26	1	1.26			
Linear vs Mean	0.0161	3	0.0054	0.8901	0.4675	
2FI vs Linear	0.0094	3	0.0031	0.4650	0.7116	
Quadratic vs 2FI	0.0857	3	0.0286	195.10	< 0.0001	Suggested
Cubic vs Quadratic	0.0008	4	0.0002	1.80	0.2469	Aliased
Residual	0.0007	6	0.0001			
Total	1.37	20	0.0686			

The sequential model sum of squares table illustrates how the model fit becomes better as more terms are added. The highest order polynomial where the additional terms are significant and the model is not aliased was chosen as the best fit based on the estimated sequential model sum of squares. Because the cubic polynomial was aliased, it was determined that it could not be used to fit the final model from the results of table 2. Additionally, it was suggested that the quadratic and 2FI model suited the data the

best, which supported the adoption of the quadratic polynomial in this research.

The lack of fit test was estimated for each answer in order to assess how well the quadratic model can account for the underlying variation present in the experimental data. Prediction cannot be made using a model with a considerable lack of fit. Table 2 displays the findings of the computed lack of fit for the typical weight reduction.

Table 2: Lack of fit test for Average Weight Loss

Source	Sum Squares	of df	Mean Square	F-value	p-value	
Linear	0.0961	11	0.0087	131.11	< 0.0001	
2FI	0.0868	8	0.0108	162.74	< 0.0001	
Quadratic	0.0011	5	0.0002	3.39	0.1032	Suggested
Cubic	0.0003	1	0.0003	4.97	0.0763	Aliased
Pure Error	0.0003	5	0.0001			

Table 3 shows the model statistics calculated for the typical weight loss response based on the model sources.

Table 3: Model summary statistics for Average Weight Loss

Source	Std. Dev.	R ²	Adjusted R ²	Predicted R ²	PRESS	
Linear	0.0777	0.1430	-0.0177	-0.2738	0.1434	
2FI	0.0819	0.2261	-0.1311	-0.7097	0.1925	
Quadratic	0.0121	0.9870	0.9753	0.9189	0.0091	Suggested
Cubic	0.0105	0.9941	0.9813	0.3472	0.0735	Aliased

The summary statistics concerning model fit encompass various metrics such as standard deviation, R-squared, adjusted R-squared, predicted R-squared, and the predicted error sum of squares (PRESS) statistic for each complete model. In this context, an ideal model is characterized by a low standard deviation, an R-squared value close to one, and a relatively low PRESS. Accordingly, based on the findings detailed in Table 3, the

quadratic polynomial model is recommended, while it should be noted that the cubic polynomial model was deemed unsuitable due to aliasing issues.

This choice of the quadratic polynomial model is further validated by assessing its ability to minimize average weight loss, as elaborated in the goodness-of-fit statistics presented in Table 4.

Table 4: GOF statistics for Average Weight Loss

Std. Dev.	0.0121	R²	0.9870
Mean	0.2510	Adjusted R²	0.9753
C.V. %	4.82	Predicted R²	0.9189
		Adeq Precision	27.3202

The reasonably close agreement between the Predicted R², standing at 0.9189, and the Adjusted R², which is 0.9753, is noteworthy, with the difference between them falling comfortably below the 0.2 threshold. Moreover, the signal-to-noise ratio, as quantified by Adeq Precision, is notably favorable, registering at 27.320, well surpassing the desired ratio of 4. This signifies that the model is sufficiently robust

and reliable for guiding explorations within the design space.

A juxtaposition between the projected values and the actual values was done in order to find values or groupings of values that the model would not have been able to detect readily. This comparison is shown in Figure 1, with a special emphasis on the average weight loss.

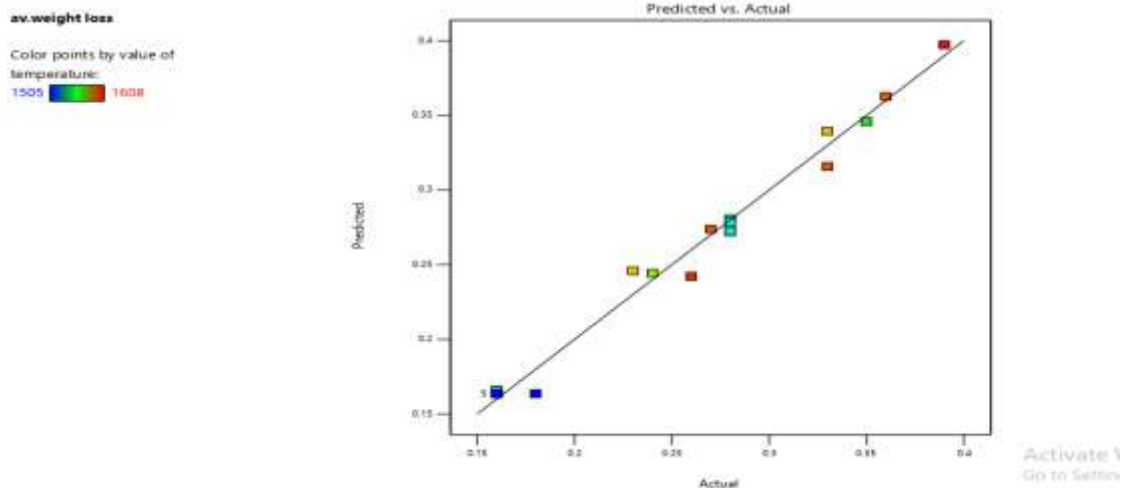


Figure 1: Plot of Predicted Vs Actual for Average Weight Loss

The graph in Figure 1 shows how the dots are closely grouped around the fitted line. This shows that the model is successful in correctly predicting the bulk of the data points.

A Cook's distance plot was created for various responses in the experimental data to

look for probable outliers. Cook's distance estimates how the removal of a certain point can affect the regression. In order to rule out outliers, points with extremely elevated distance values in comparison to the rest should be given more attention. Figure 2 shows the Cook's distance plot for the average weight loss.

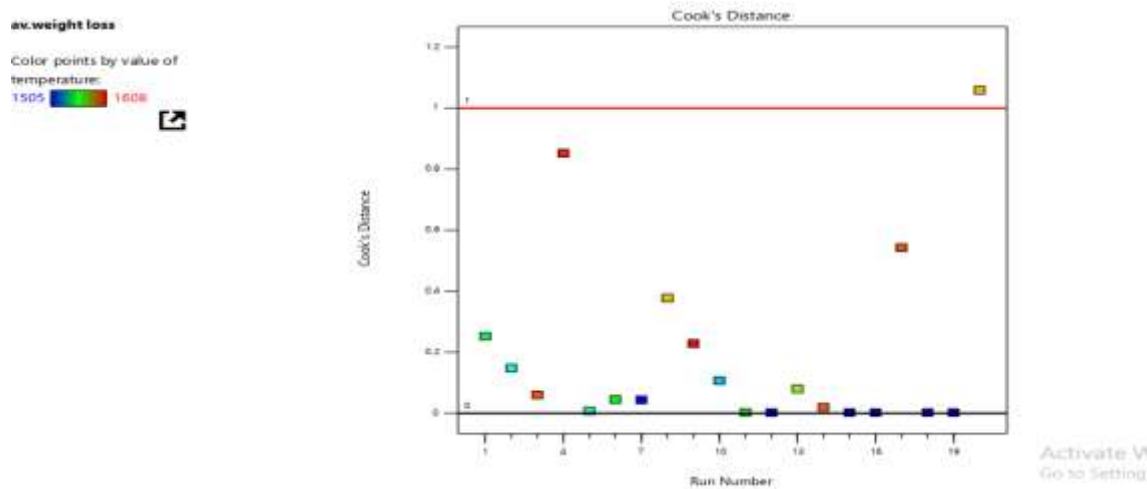


Figure 2: Generated cook's distance for Average Weight Loss

The Cook's distance plot, on the other hand, is shown in Figure 2, and it has 0.00 for the lower bound and 1.00 for the upper bound. Outliers are considered experimental values

that are outside the expected range and require further examination. The results of Figures 1 and 2 imply that the

estimated residuals follow a distribution that is roughly normal. This is a good sign because it shows that the constructed model's accuracy and propensity for prediction are sufficient.

Figure 3 shows 3D surface plots analyze the effects of voltage and current on the average weight loss while Figure 4 illustrates 3D surface plots were created to explore the effects of average weight loss on current and gas flow rate.

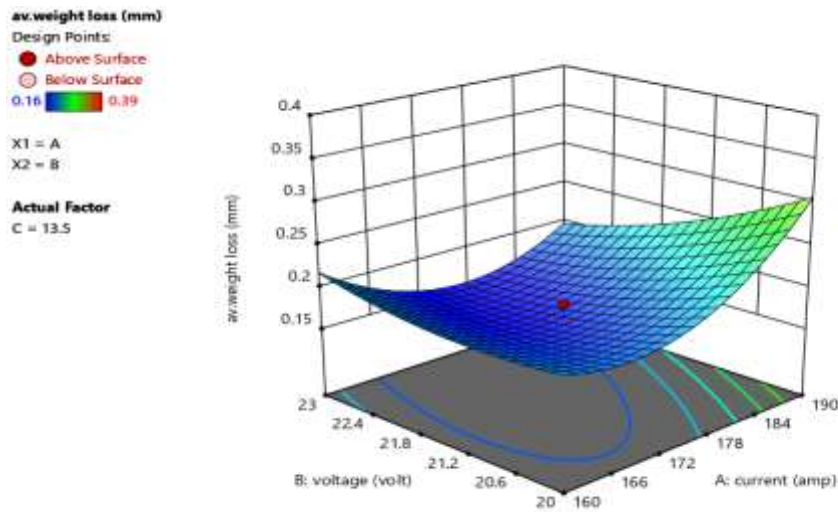


Figure 3: Effect of voltage and gas flow rate on AWL

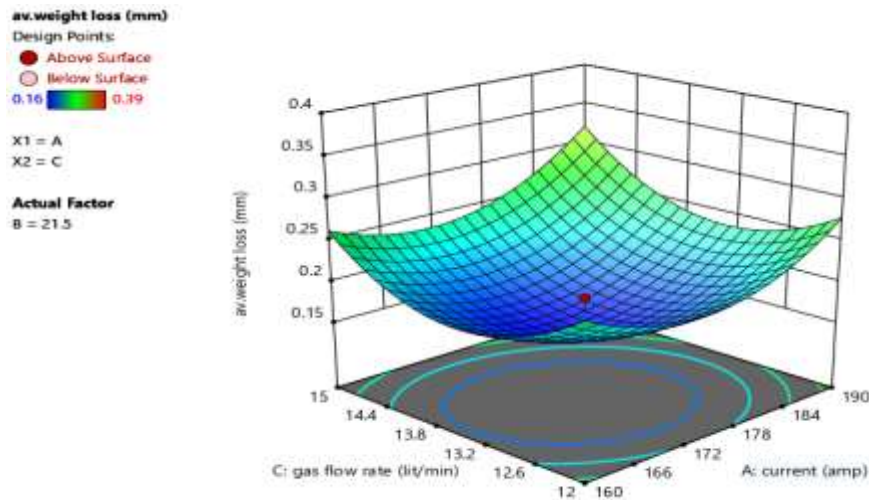


Figure 4: Effect of current and gas flow rate on AWL

*Corresponding author, e-mail:author@fupre.edu.ng

The 3D surface plots shown in Figure 5 were created as follows to explore the impacts of voltage and gas flow rate on the average weight loss. Figure 6 shows the contour plots

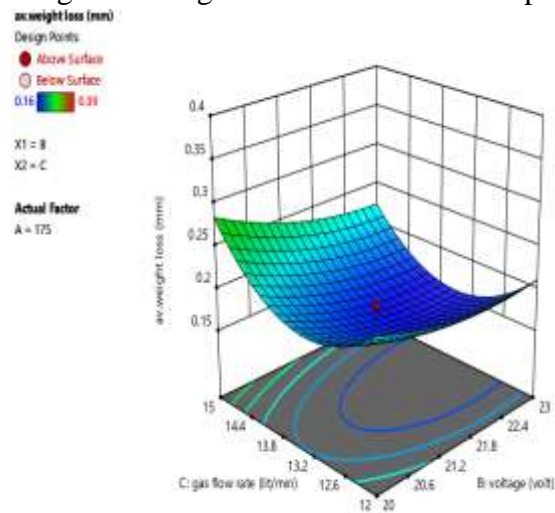


Figure 5: Effect of voltage and gas flow rate on AWL contour plot

of the average weight loss response variable against the optimal value of current and voltage.

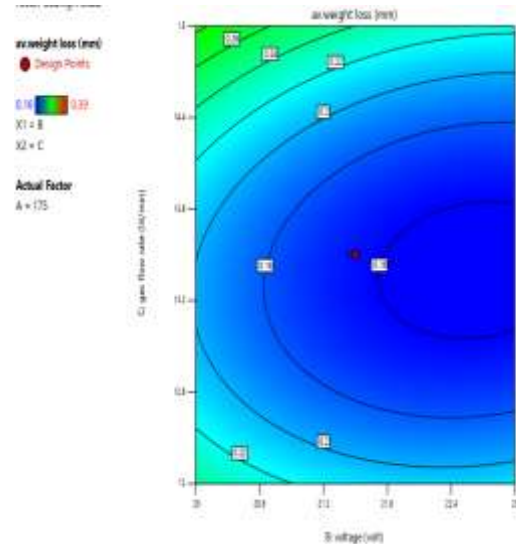


Figure 6: Predicting AWL using contour plot

3.1.2 Modelling of Weight Loss using Artificial Neural Network (ANN)

The examination also held vital value in establishing the precise mathematical link between the input parameters (current, voltage, and gas flow rate) and the outcome parameter (weight loss). In the pursuit of attaining an optimal network structure that provides the highest precision in comprehending the input-output data correlation, two pivotal aspects were taken into account. The initial aspect encompassed choosing the most precise training algorithm or learning rule. Furthermore, the determination of the number of hidden neurons within the network was also contemplated. Guided by these considerations, a variety of training algorithms and different quantities of hidden neurons were chosen and subjected to experimentation. The aim was to identify the

optimal training algorithm and the optimal number of hidden neurons that collaboratively yield the most accurate and efficient network configuration. However, this selection is based on the assessment of r^2 and MSE values. For the analysis of the Artificial Neural Network, MATLAB R2022a was employed. The data was initially saved in a specific MATLAB folder, after which it underwent normalization by being converted into a numeric matrix. This process automatically established the dataset range, and the import selection was employed to import the data into the MATLAB environment.

The Levenberg-Marquardt Back Propagation training algorithm, known as the improved second-order gradient method, has been identified as the optimal learning rule and subsequently applied in formulating the network structure. The process of network

*Corresponding author, e-mail:author@fupre.edu.ng

generation involved partitioning the input data into sets for training, validating, and testing. In this investigation, 70% of the data was allocated for network training, 15% for validation, and the remaining 15% for testing. The evaluation of the network's performance

extended over a maximum of 1000 training epochs. By implementing these parameters and configurations, an optimal neural network structure was established and visually represented in Figure 7.

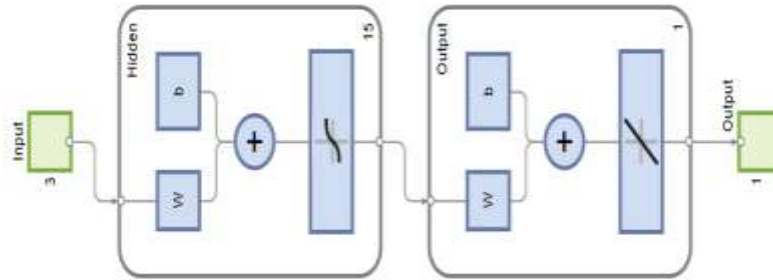


Figure 7: Artificial neural network architecture

The network diagram created utilizing the back propagation neural network and the

artificial neural network architecture 3-15-1 to predict weight loss is shown in Figure 8.



Figure 8: Model summary for predicting weight loss

Figure 9's network training diagram revealed that the network performance was of 0.0773

Validation check of two (2) was recorded out of six (6). However, this is to be expected

given that the raw data's normalization resolved the weight bias issue. Figure 9 displays a performance evaluation plot that depicts the development of training, validation, and testing. The network's effectiveness during each of these stages is shown visually in this plot. The training state

is shown in Figure 10, which provides details on important variables like the gradient function, training gain (Mu), and validation tests. The training process and its connected aspects are clearly understood thanks to this thorough representation.

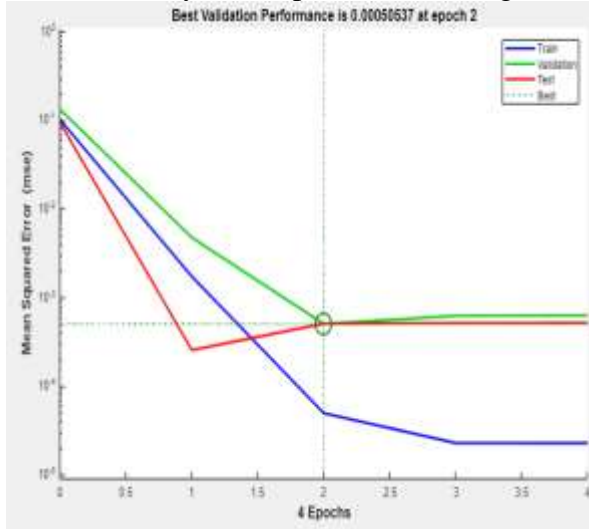


Figure 10: Performance curve for predicting AWL

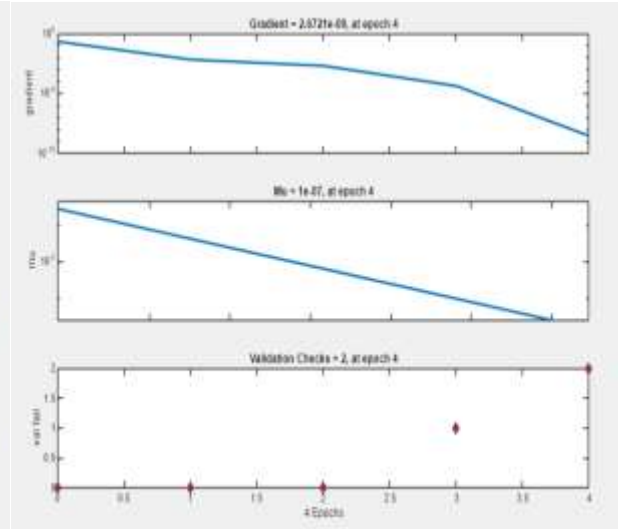


Figure 11: Neural network training for predicting AWL

Backpropagation is a fundamental technique employed within artificial neural networks to compute the error contribution of each neuron following a batch of data training. In technical terms, the neural network calculates the gradient of the loss function to elucidate the extent of error attributed to each of the selected neurons. In this context, lower error values are indicative of superior performance. The computed gradient value, notably small at 0.000000002672 as depicted in Figure 11, signifies that the error contributions from these selected neurons are exceedingly minimal. Momentum gain (Mu) serves as the pivotal control parameter for the neural

network training algorithm. It plays a crucial role in shaping the network's learning dynamics, and its value must be maintained below unity to ensure stability. The utilization of momentum gains set at 0.0000001 underscores the network's remarkable capacity for accurately predicting weight loss. The regression plot, featured in Figure 12, effectively illustrates the correlation between the input variables (current, voltage, and gas flow rate) and the target variable (weight loss). It concurrently showcases the progression of training, validation, and testing phases, providing a comprehensive view of the model's performance throughout the different stages of its development and evaluation.

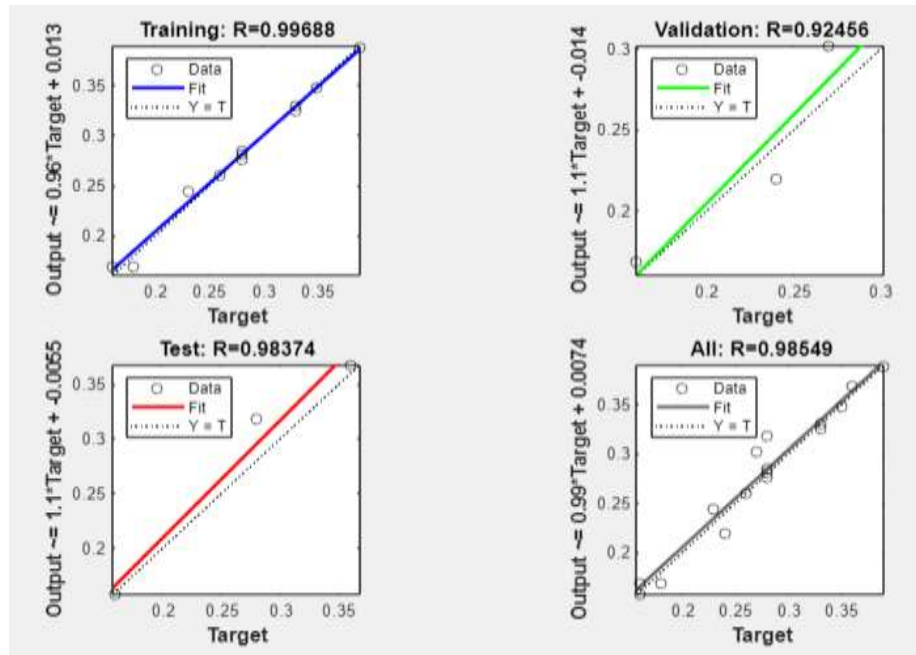


Figure 12: Regression plot showing the progress of training, validation and testing

The network has been accurately trained and can be used to forecast weight loss, according to computed values of the correlation coefficient (R) as seen in Figure 12.

3.2. Discussion of Result Findings

The Response Surface methodology and artificial neural network techniques were utilized in this study to anticipate and optimize the average weight loss of Tungsten inert gas mild steel welds. The input parameters are current, voltage and gas flow rate while the response is the average weight loss. The connection between the parameters used as input and the outcome happens to be quadratic, as the sequential sum of square test for the response selected the quadratic model which has a p-value < 0.0001 . The model summary statistics for all the responses have R^2 values of about 90% and the models have non-significant lack of fit with p-value > 0.005 . The models all have R^2 values > 0.9 indicating the strength and how well the model can determine the values of the chosen

input variables in advance that will predict the best values of responses for a very good weld, the results obtained showed that the variance inflation factor (VIF) was 1.00 which is expected. Design experts determined that this option, which has a desirability rating of 0.918, is the best one. The study reveals the successful use of artificial neural networks in predicting the average weight loss for tungsten inert gas welding of mild steel plates.

4. CONCLUSION

The average weight loss of a fabricated engineering structure is a critical factor affecting its usable service life. In this research, the development of numerical models using response surface methodology and artificial neural network to optimize and predict the average weight loss, considering current, voltage and gas flow rate as input factors. The experimental design adopted was the central composite design, which was generated using the design expert software

(version 13.0) the RSM analysis produced optimal solutions with current of 160.000 amps, voltage of 21.280 volts, gas flow rate of 14.667lit/min to produce a welded joint with average weight loss of 0.236 and this was obtained at a desirability value of 0.918. The artificial neural network model was also employed to predict the output parameters and compared with the RSM methodology. From the results obtained the Response Surface Methodology is selected as the better predictive model over the Artificial Neural Network because it has a higher coefficient of determination.

References

- Alzeer, M. B., Ghorayeb, K., & Mustapha, S. (2023). Transportation Pipelines Corrosion: The Roles Played by Pressure, Metallurgy, and Geography. *Procedia Structural Integrity*, 48, 363-370.
- Ardil, C. (2023). Using the PARIS Method for Multiple Criteria Decision Making in Unmanned Combat Aircraft Evaluation and Selection. *International Journal of Aerospace and Mechanical Engineering*, 17(3), 93-103.
- Cecchel, S. (2021). Materials and Technologies for Light weighting of Structural Parts for Automotive Applications. *SAE International Journal of Materials and Manufacturing*, 14(1), 81-98.
- Cheng, A., & Chen, N. Z. (2022). Structural integrity assessment for deep-water subsea pipelines. *International Journal of Pressure Vessels and Piping*, 199, 104711.
- Dogra, V. (2018). Application of Welding Process Parameters Using AI Algorithm. *Turkish Journal of Computer and Mathematics Education (TURCOMAT)*, 9(2).
- Fernandes, R. F., Jesus, J. S., Branco, R., Borrego, L. P., Costa, J. D., & Ferreira, J. A. M. (2022). Influence of post-processing heat treatment on the cyclic deformation behaviour of AlSi10Mg aluminium alloy subjected to laser powder bed fusion. *International Journal of Fatigue*, 164, 107157.
- Jiang, X. (2018, June). Structural integrity assessment of maritime transport equipment. In *International Conference on Offshore Mechanics and Arctic Engineering* (Vol. 51333, p. V11BT12A033). American Society of Mechanical Engineers.
- Li, J., Li, H., Liang, Y., Liu, P., Yang, L., & Wang, Y. (2020). Effects of heat input and cooling rate during welding on intergranular corrosion behavior of high nitrogen austenitic stainless steel welded joints. *Corrosion Science*, 166, 108445.
- Li, X., Chen, G., Chang, Y., & Xu, C. (2019). Risk-based operation safety analysis during maintenance activities of subsea pipelines. *Process Safety and Environmental Protection*, 122, 247-262.
- Linda, L. S., & Pistorius, P. G. H. (2022). Effect of titanium content on solidification structure of ferritic stainless-steel gas-tungsten and gas-metal arc welds. *Journal of the Southern African Institute of Mining and Metallurgy*, 122(7), 331-336.
- Liu, M. A. (2021). *Analyses of Compositionally-Graded Co-Cr-Mo Processed by Directed Energy*

Deposition (Doctoral dissertation, Texas A&M University).

- Miranda, D. A. D., & Nogueira, A. L. (2019). Simulation of an injection process using a CAE tool: Assessment of operational conditions and mold design on the process efficiency. *Materials Research*, 22.
- Sabdin, S. D., Hussein, N. I. S., & Sued, M. K. (2019). A Review on Thin Plates Joining Method Using Arc Welding as The Heat Sources. *Journal of Industry, Engineering and Innovation*, 1(2).
- Seyfipour, I., Mirghaderi, R., & Bahaari, M. R. (2023). Buckling and stability of subsea HP/HT pipelines on laterally sloping seabeds. *Journal of Ocean Engineering and Marine Energy*, 9(1), 1-23.
- Spoerk, M., Holzer, C., & Gonzalez-Gutierrez, J. (2020). Material extrusion-based additive manufacturing of polypropylene: A review on how to improve dimensional inaccuracy and warpage. *Journal of Applied Polymer Science*, 137(12), 48545.
- Zhao, J., Qiu, F., & Xu, C. (2023). Review of Creep-Thermomechanical Fatigue Behavior of Austenitic Stainless Steel. *Crystals*, 13(1)